

CHAPTER 5: HIGH RESOLUTION SEDIMENTOLOGICAL  
STUDIES

## 5.1 Introduction

Sedimentological characters of river bank deposits and their formative processes are studied by researchers all over the world (Steiger et al., 2001; Gregory et al., 2006; Wang et al., 2006; Provansal et al., 2010). The principle underlying assumption in such studies is “distribution of grain size in a sedimentary sequence is the reflection of mechanisms involved in sediment transport and its depositional environment”. There are number of statistical methods for analysing grain size record determining depositional environments (Krumbein, 1934; Passega, 1964; Sahu, 1964; Folk, 1966; Friedman, 1967; Doeglas, 1968; Visher, 1969; Guerzoni et al., 1996; Pandey et al., 2002; Richard et al., 2005; Blott and Pye, 2006; Purkait, 2006; Bartholdy et al., 2007; Ren and Packman, 2007; Cheetham et al., 2008; Goossens, 2008; Poizot et al., 2008; Brandono et al., 2009; Buscombe and Masselink, 2009; Citterio and Piegay, 2009; Oldfield et al., 2009; Smith et al., 2009; Zervas et al., 2009; Hajek et al., 2010).

Such quantitative study on high resolution is attempted for first time to decode 802 cm thick sediment sequence, representing significant landform “Uchediya surface” in the LrNV. Previously the studies were carried out in the region, in relation with geomorphology and neotectonic implications, stratigraphy and depositional environments based on visual interpretation and analysis of few representative samples for determining sediment facies, clay mineralogy, chronology and palynology. (Allchin and Hegde, 1969; Gadekar et al., 1981; Bedi and Vaidyanadhan, 1982; Babu, 1984; Karanth et al., 1988b; Sundaram et al., 1991; Sant and Karanth, 1993; Chamyal et al., 2002; Bhandari, 2004b; Bhandari et al., 2005; Raj, 2007; Raj and Yadava, 2009; Sridhar and Chamyal, 2010). The aforesaid studies gives overall understanding of LrNV, however, in depth study is called for understanding channel morphology for last 500 years. In the present work, an

attempt is made to determine high resolution quantitative sediment facies, understand trends in facies change and energy conditions associated with sediment facies implying to climate phase within late Holocene.

## 5.2 Methodology

The samples collected from the neobank of the Uchediya surface along Narmada channel near Uchediya village were subjected to grain size analysis. Particle size distribution was determined using long established sieve-pipette method (Folk, 1974; Cheetham et al., 2008). A hundred gram split of each sample were separated from the total sample by the method of coning and quartering. These samples were treated with dil. HCl and 6% hydrogen peroxide followed by washing with distilled water to remove carbonate and organic matter from the sample. After washing and cleaning, samples were subjected to wet sieving through 63  $\mu$  sieve to separate silt and clay sediments. Greater than 63  $\mu$ m sediments were then ran in sieve shaker using sieves of 1000  $\mu$ m, 400  $\mu$ m, 250  $\mu$ m, 210  $\mu$ m, 149  $\mu$ m, 125  $\mu$ m, 105  $\mu$ m, 88  $\mu$ m, 74  $\mu$ m and 63  $\mu$ m. Each fraction was then collected separately and packed in aluminium foil and further in air tight bags. The samples were weighed on Mettler electronic weighing balance of 0.001g precession.

Less than <63  $\mu$ m sediment fraction were used for pipette analysis. 10 gm of sample put into the cylinder along with some amount of distilled water, 1ml of 10% collagen solution that was finally made up to 1000ml. The experimental cylinder was then put in a water bath to maintain the uniform temperature throughout the experiment. After stirring the cylinder rigorously for 2-3 minutes, pipetting is done at calculated time intervals for 31  $\mu$ m, 16  $\mu$ m, 8  $\mu$ m, 4  $\mu$ m and 2  $\mu$ m respectively using Stock's law. Each fraction was oven dried and carefully

weighed. Weight percentages for all 15 fractions were calculated and used for determining various sedimentological parameters and quantitative sediment facies.

Table 5-: Equations and terminologies used for the statistical analysis.

Graphic Mean (M)		Graphic Sorting ( $\sigma_1$ )		Graphic Skewness ( $Sk_1$ )		Graphic Kurtosis ( $K_G$ )	
$\frac{\phi_{16} + \phi_{50} + \phi_{84}}{3}$		$\frac{\phi_{84} - \phi_{16}}{4} + \frac{\phi_{95} - \phi_5}{6.6}$		$\frac{\phi_{16} + \phi_{84} - 2\phi_{50}}{2(\phi_{84} - \phi_{16})} + \frac{\phi_5 + \phi_{95} - 2\phi_{50}}{2(\phi_{95} - \phi_5)}$		$\frac{\phi_{95} - \phi_5}{2.44(\phi_{75} - \phi_{25})}$	
Very coarse sand	-1 to 0	Very well sorted	<0.35	Very fine skewed	+0.3 to +1.0	Very platykurtic	<0.67
Coarse sand	0 to 1	Well sorted	0.35-0.50	Fine skewed	+0.1 to +0.3	Platykurtic	0.67-0.90
Medium sand	1 to 2	Moderately well sorted	0.5- 0.70	Symmetrical	+0.1 to -0.1	Mesokurtic	0.90-1.11
Fine sand	2 to 3	Moderately sorted	0.70- 1.00	Coarse skewed	-0.1 to -0.3	Leptokurtic	1.11-1.50
Very Fine sand	3 to 4	Poorly sorted	2.00	Very coarse skewed	-0.3 to -1.0	Very leptokurtic	1.50-3.00
Very coarse silt	4 to 5	Very poorly sorted	2.00- 4.00			Extremely leptokurtic	>3.00
Coarse silt	5 to 6	Extremely poorly sorted	>4				
Medium silt	6 to 7						
Fine silt	7 to 8						
Very Fine silt	8 to 9						

The grain size distribution record (401 samples and 15 grain size fraction for each sample) are ran through statistical package GRADISTAT v6 (Blott and Pye, 2001) to determine sedimentological parameters viz., Graphic Mean ( $\phi$ ) Graphic Sorting ( $\sigma_1$ ), Graphic Skewness ( $Sk_1$ ) and Graphic Kurtosis ( $K_G$ ). The parameters are calculated using the equations by Folk and Ward (1957) (Table 5-). However, the descriptive terminology of Skewness, instead of Positive skewness and Negative Skewness, the present section uses 'Fine Skewed' and 'Coarse Skewed' for sediments of excessive fine sediments and excessive coarse sediments respectively (After Blott and Pye, 2001). In view of bimodal and polymodal sediments, the Graphic Standard Deviation (Sorting), Graphic Skewness and Graphic Kurtosis of sediments are considered for qualitative comparison along the vertical sequence only.

### 5.3 Sediment facies

In the present study, the sequence is classified into two broad sedimentary facies namely Sandy facies (68%) and muddy facies (32%). Each of the facies is subdivided into subfacies based on cluster analysis of granulometric data for 401 samples.

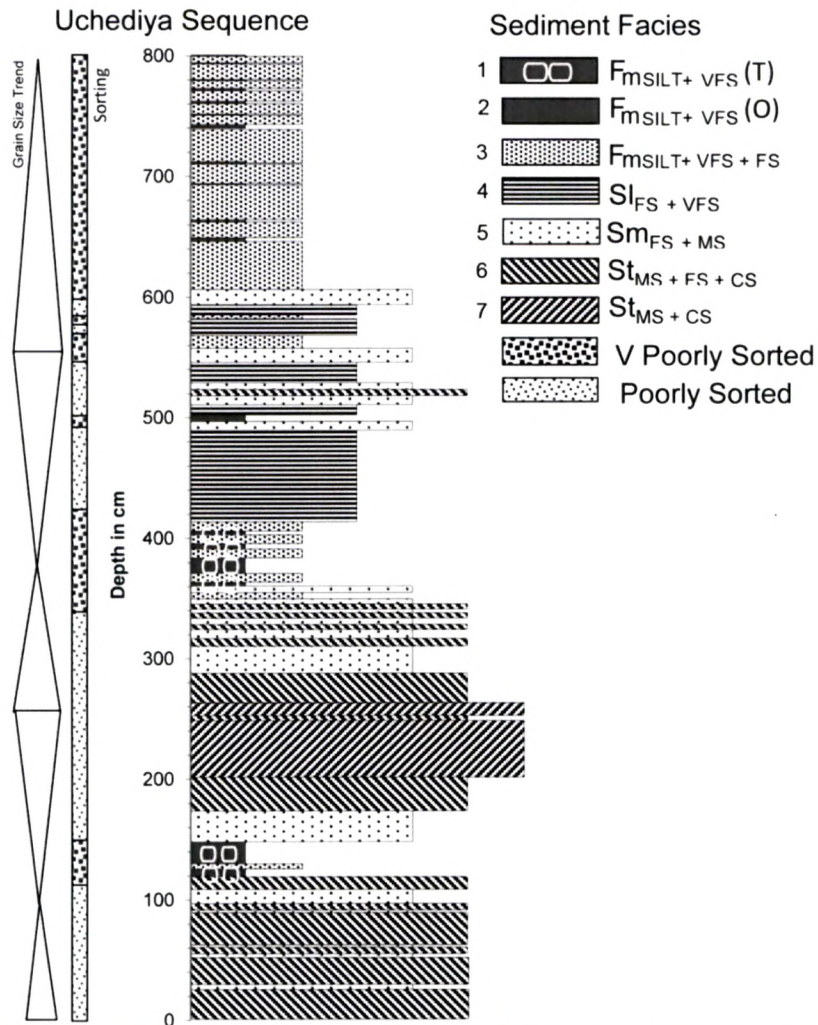


Figure 5-: Litholog of Uchediya sequence showing different sedimentary subfacies and their associations

Each cluster was quantitatively determined, compared, evaluated, and supplemented with field base details. Each cluster is referred to as sediment “subfacies” in the present study (

Figure 5- and Figure 5-). The sediment subfacies are supplemented with other supporting records on composition and micro faunal assemblages at certain

depths to resolve intricacies within subfacies. The nomenclature of sediment subfacies is in line with litho-facies classification after Martins (1965), Friedman,(1967), Jackson, (1975), Miall (1978, 1985), Friend et al., (1979), Friend et al., (1986) and Martinius, (2000).

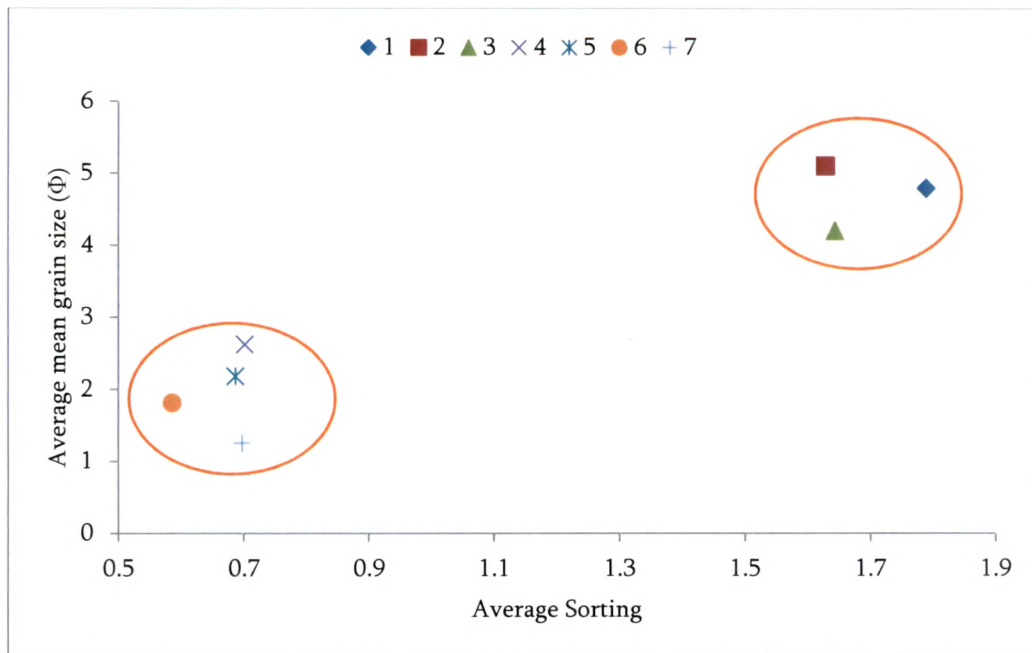


Figure 5-: Plot of average sorting against averaged mean grain size of individual facies clearly shows clustering of two groups. Numbers 1 to 7 indicate the individual facies code as same as figure 5-1

### 5.3.1 Sandy Facies

The sandy facies are the most dominant facies (68%) exposed along the Uchediya sequence. The facies are inferred based on data from 246 samples. The sand facies show both laminated and trough-shaped cross bedding structures. The sandy facies are further subdivided into four sub facies viz.,  $St_{MS+FS+CS}$  (32%),  $Sm_{FS+MS}$  (29%)  $Sl_{FS+VFS}$  (26%), and  $St_{MS + CS}$  (13%). where Sl- is laminated sand; St- trough-shaped cross bedded; and subscript represent grain size (fine sand, very fine sand, medium sand an coarse sand) (Figure 5-). In overall, the sandy facies are poorly sorted (sorting ranges from 1.26 to 2) and show modality from bimodal to unimodal distribution.

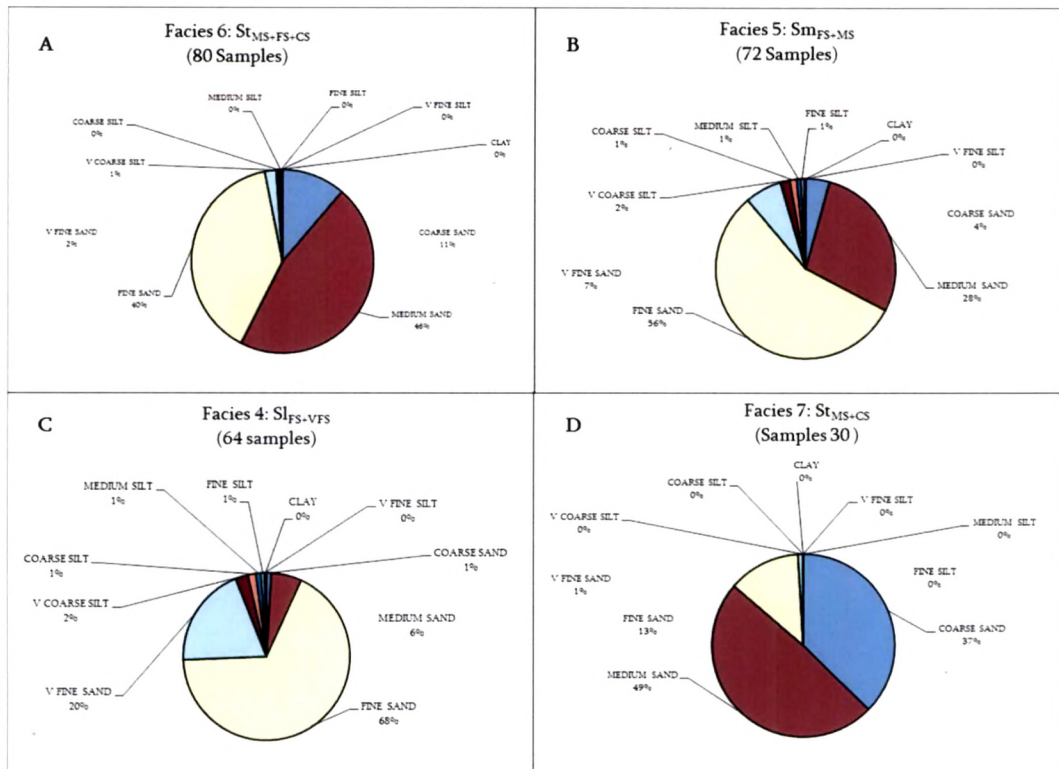


Figure 5:- Pie diagram showing average values of sand, silt and clay percentage variation in sandy sedimentary subfacies.

St<sub>MS</sub>+FS+CS sub facies (10YR 5/4 to 10YR 4/3) are decoded from analyzing around 80 samples, the sub facies constitutes 32% of total sandy facies (Figure 5-A). The sub facies shows trough-shaped cross bedding with basalt pebbles seen occasionally along the trough cross. The sub facies have developed prominently in the lower portion of the sequence between 0 to 120 cm depth. The high resolution analysis signifies the St<sub>MS</sub>+FS+CS sub facies and is sub divided into number of units by intercalation of thin (few centimeters to 10 cm) units of Sm<sub>FS</sub>+MS subfacies and thick (50 cm) unit of St<sub>MS</sub> + CS sub facies. St<sub>MS</sub>+FS+CS sub facies are moderately well sorted showing unimodal, symmetrical and platykurtic distribution.

Sm<sub>FS</sub>+MS subfacies (10YR 5/4 to 10YR 3/3) are decoded based on analysis of 72 samples and comprises of 29% of sandy facies (Figure 5-B). St<sub>FS</sub>+MS subfacies are massive in nature and occur as intercalating suite from base of the sequence up to 210 cm in the sequence. The facies become prominent at 150cm to 168cm and 290

cm to 310 cm from the base. The sediment unit with  $St_{FS+MS}$  subfacies varies in thickness from few centimeters to maximum 20 cm.  $Sm_{FS+MS}$  sub facies are moderately sorted, showing unimodal, skewed towards very fine and very leptokurtic in distribution.

$Sl_{FS+VFS}$  subfacies are decoded from analysis of 64 samples and comprise 26% of the sandy facies (Figure 5-C).  $Sl_{FS+VFS}$  subfacies (10YR 5/4 to 10YR 4/5) are laminated and seen restricted in the central portion of the sequence between 415 cm to 485 cm. The sub facies also occur as intercalating suite alternate with its coarser equivalents from depth of 500 cm to 590 cm.  $Sl_{FS+VFS}$  sub facies are moderately sorted showing bimodal nature skewed towards very fine classes showing very fine skewed and leptokurtic.

$St_{MS+CS}$  subfacies (10YR 5/4 to 10YR 4/3) are decoded from analysis of 30 samples respectively and comprises of 13% of sandy facies (Figure 5-D).  $St_{MS+CS}$  sub facies also shows trough-shaped cross bedding identified occurring within the  $St_{MS+FS+CS}$  sub facies as a coarser fraction from 200 cm to 245 cm.  $St_{MS+CS}$  sub facies differs from  $St_{MS+FS+CS}$  sub facies with very platykurtic nature of distribution curve.

### 5.3.2 Muddy Facies

The muddy facies are the second dominant facies (32%) exposed along the Uchediya sequence. The facies is inferred based on data from 155 samples. The muddy facies show both massive and laminated in nature. Overall the muddy facies is very poorly sorted (sorting ranges from 3.1 to 3.3). Based on the quantitative analysis of grain size data and association of primary structures within the muddy facies are further subdivided into two sub facies namely,  $Fm_{SILT+VFS}$  and  $Fm_{SILT+VFS+FS}$  where  $Fm$ -is massive muddy subfacies;  $Fl$ -is laminated muddy subfacies; and subscript represent dominance of grain size (silt, very fine sand and fine sand).  $Fm_{SILT+VFS+FS}$  subfacies are poorly sorted showing bimodal to trimodal very fine skewed, platykurtic distribution, however the facies is subdivided into

Fm<sub>SILT+VFS</sub> (O) and Fm<sub>SILT+VFS</sub> (T) subfacies based on the presence (T) or absence (O) of microfossil assemblage in the different levels (Chapter 6).

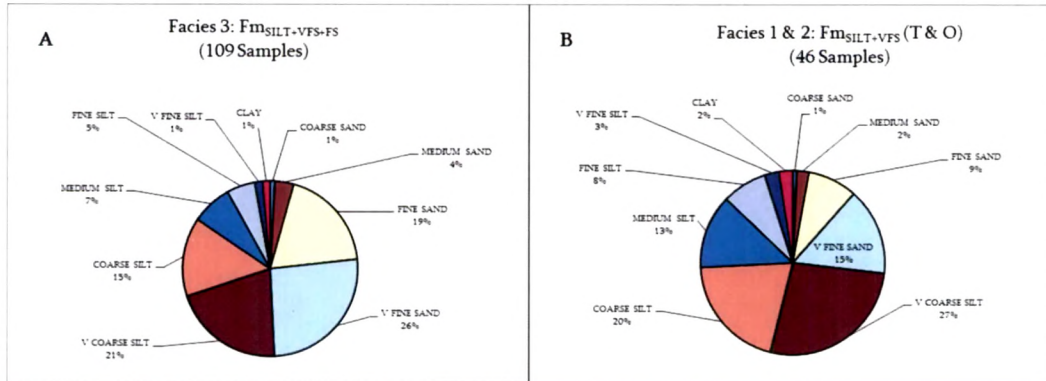


Figure 5-: Pie diagram showing average values of sand, silt and clay percentage variation in muddy sedimentary subfacies

Fm<sub>SILT+VFS+FS</sub> subfacies (10YR 4/4 to 10YR 4/3) are decoded from analysis of 109 samples respectively (Figure 5-A) comprising 71% of the muddy facies. The Fm<sub>SILT+VFS+FS</sub> subfacies dominate in the sequence from 605 cm to 802 cm depth. A single unit varies from maximum 35cm to few centimeters. The sub facies unit thins consistently upwards.

Fm<sub>SILT+VFS</sub> sub facies (10YR 4/4 to 10YR 4/3) are decoded from analysis of 46 samples comprising 29% of muddy facies (Figure 5-B). Fm<sub>SILT+VFS</sub> sub facies units are well developed at depths from 120 cm to 145cm, 360 cm to 410cm, 495 cm to 500 cm and 605 cm to 802 cm. Fm<sub>SILT+VFS</sub> sub facies occur as a thin intercalating unit with Fm<sub>SILT+VFS+FS</sub> sub facies from 605 cm to 802 cm and vice versa at depths between 120 cm to 145cm and 360 cm to 410cm. Based on presence or absence of foraminiferal assemblage the present study further classify Fm<sub>SILT+VFS</sub> subfacies into Fm<sub>SILT+VFS</sub> (O) and Fm<sub>SILT+VFS</sub> (T) representing overbank and tidal conditions respectively.

## 5.4 Palaeohydrology

The grain size distribution in a sedimentary sequence gives quantitative textural characteristic for suites of facies. Various statistical parameters further capture the mechanism of sediment transport, the environment of deposition and its changes (Krumbein, 1934; Passega, 1964; Sahu, 1964; Folk, 1966; Friedman, 1967; Doeglas, 1968; Visher, 1969; Guerzoni et al., 1996; Pandey et al., 2002; Richard et al., 2005; Purkait, 2006; Bartholdy et al., 2007; Ren and Packman, 2007; Cheetham et al., 2008; Goossens, 2008; Poizot et al., 2008; Brandono et al., 2009; Buscombe and Masselink, 2009; Citterio and Piegay, 2009; Oldfield et al., 2009; Hajek et al., 2010).

Various statistical parameters calculated from the grain size distribution data viz., Mean ( $\phi$ ) Sorting ( $\sigma_1$ ), sorting within weight percentage of tails of fines (4phi and finer), Skewness ( $Sk_1$ ), Kurtosis ( $K_G$ ) after Tenner, (2007). These are further plotted to good advantage on bivariate diagrams for reasonable interpretations. These diagrams capture hydrodynamics, sediment supply, trapping and other dynamical conditions. The present study used various diagrams to differentiate transporting agencies, transitions from one agency to another, or change in energy conditions, or sediment contribution from outside systems. In view of bimodal and polymodal sediments in the different facies, the statistical parameters were used only for the relative variation in the vertical sequence of the sediment characteristics.

## 5.5 Bivariate plots

The plot of mean phi size verses weight percentage of  $<3\Phi$  sediments (Figure 5-A) shows that it is similar to segmented cumulative frequency curve, in which, each transported by a particular mechanism such as suspension load(muddy facies); saltation (Muddy and sandy facies) and traction (sandy facies).

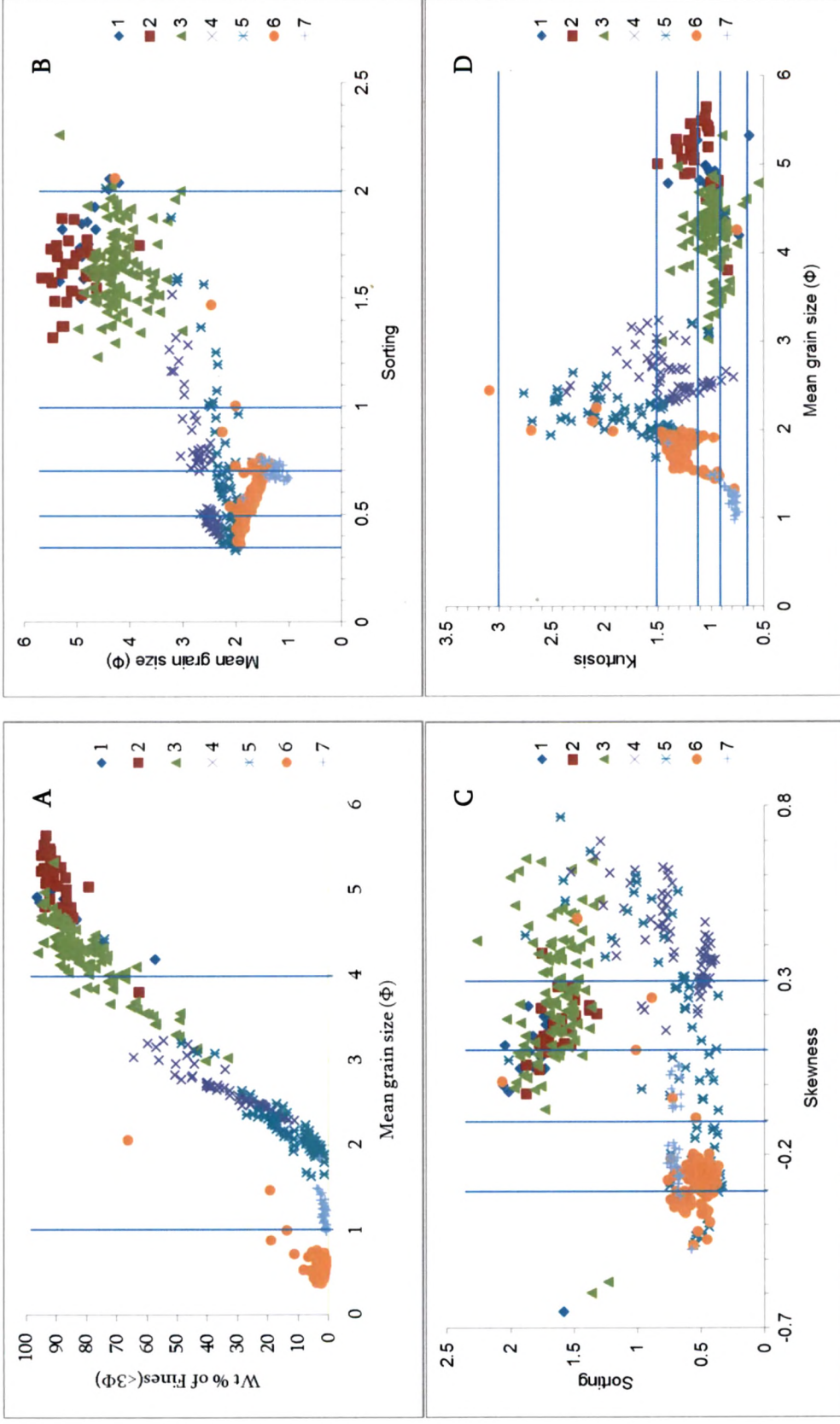


Figure 5-: Bivariate plots of 401 samples used for the characterization of sediments. Numbers 1 to 7 indicate the facies code as in Fig.5.2 and Fig.5.1.

The plot show systematic transition of facies from leading, flat upper segment to central steeper segment to trailing flat segment.  $F_{MSILT+VFS}$  (T) that leads the upper segment followed by  $F_{MSILT+VFS}$  (O) suggesting subfacies were deposited under suspension mode. The sub facies  $F_{MSILT+VFS+FS}$ , falls at the transition of upper and steeper segment of the S curve showing at least part of sub facies were under suspension and saltation.  $Sl_{FS+VFS}$ , and  $Sm_{FS+MS}$ , falls along the bottom portion of steeper segment suggesting at least part of sediment were deposited under saltation and traction.  $St_{MS+FS+CS}$  and  $St_{MS+CS}$  trails along the trailing segment indicating sediment transportation under traction. The plot clearly shows relationship between sub facies and mode of transport and thereby energy conditions at the time of deposition.

The plot between standard deviation in the grain size (sorting) and mean grain size (Figure 5-B) differentiates muddy and sandy facies where show compared to sandy facies muddy facies are poorly to very poorly sorted. The part of sub facies  $Sm_{FS+MS}$  and  $Sl_{FS+VFS}$  falls in transition (moderate to poor sorting) between muddy facies and  $St_{MS+FS+CS}$  and  $St_{MS+CS}$  sub facies. Similarly plot of skewness (degree of asymmetry of a frequency) and standard deviation (sorting) clearly differentiate muddy and sandy facies as well as partially differentiate  $Sl_{FS+VFS}$ ,  $Sm_{FS+MS}$  and  $St_{MS+FS+CS}$ ,  $St_{MS+CS}$  sub facies (Figure 5-C).

A plot with mean grain size and kurtosis (degree of peakedness) also differentiate between discussed sediment subfacies however the plot distinguish part of  $Sm_{FS+MS}$ , and  $Sl_{FS+VFS}$  showing very Leptokratic distribution where they are extremely peaked having better sorting at center then tails (Figure 5-D).

## 5.6 Other plots

The plots of Mean ( $\phi$ ) Sorting ( $\sigma_1$ ), Skewness ( $Sk_1$ ), Kurtosis ( $K_G$ ) are further plotted along the depth profile of the sequence (Figure 5-).

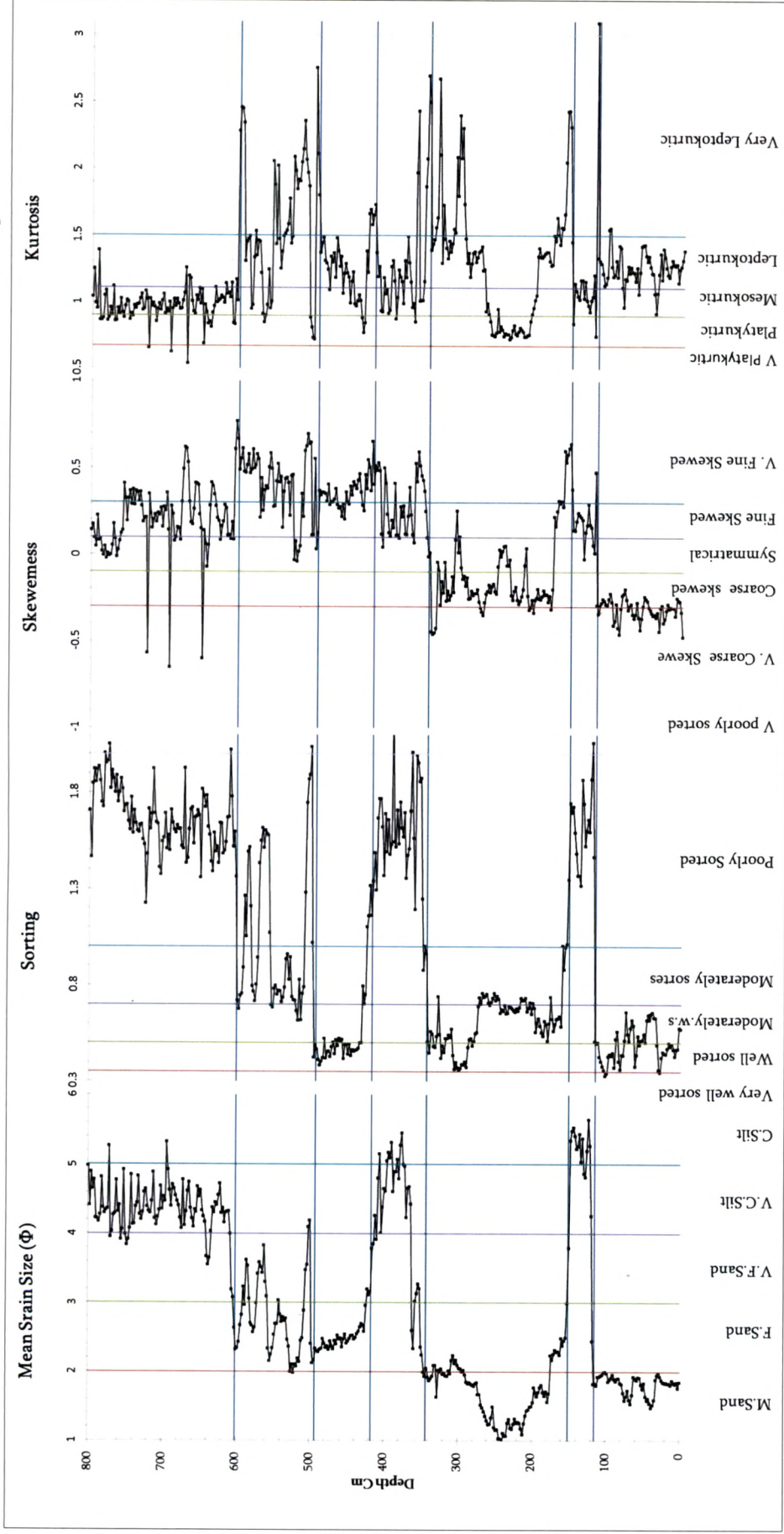


Figure 5-: Statistical parameters of Uchediya Sediments

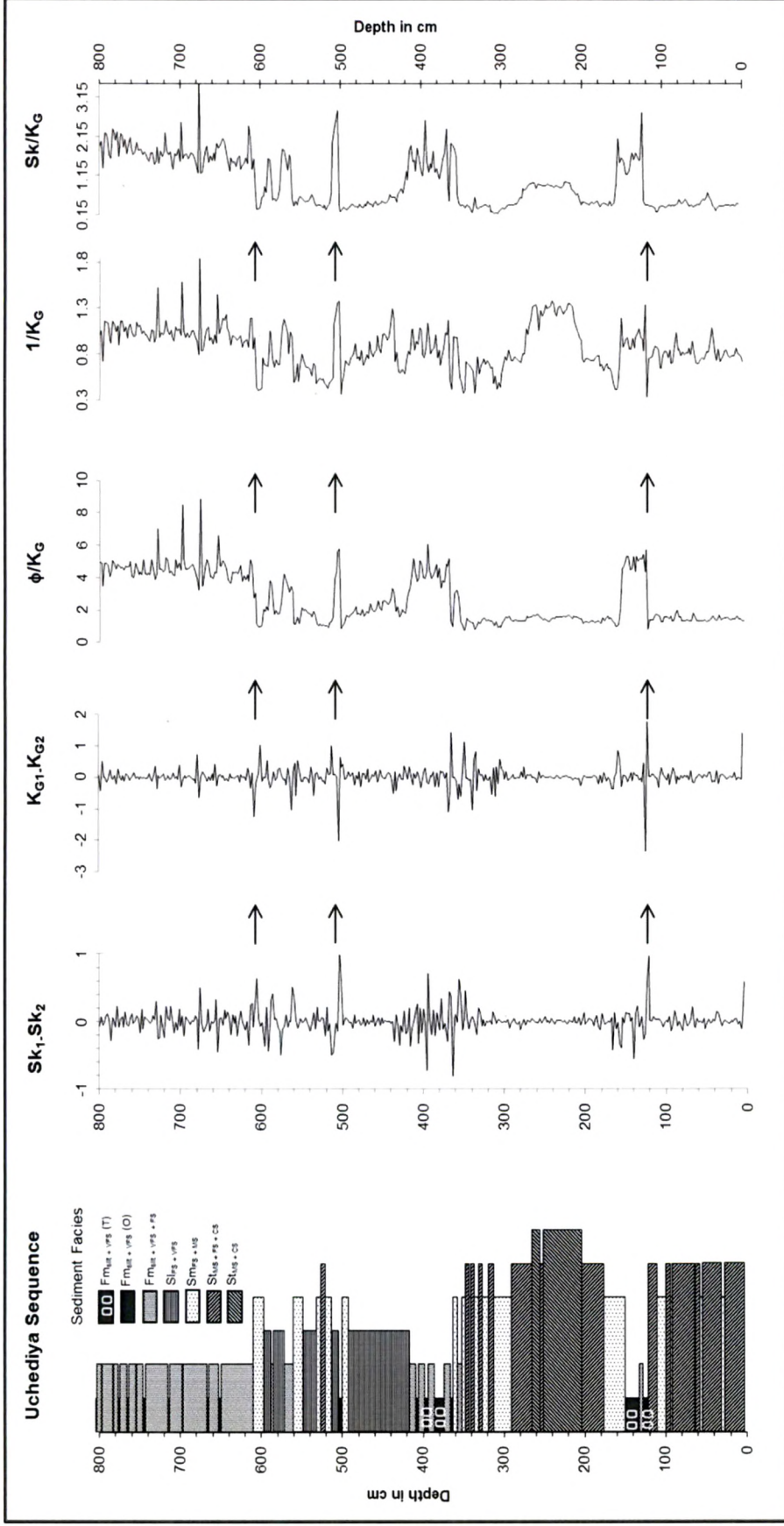


Figure 5--: Suite analysis of Uchediya sequence after Tenner, (2007). Sk1 - Sk2 and KG1-KG2 indicate the difference in skewness and Kurtosis value of successive lower and upper data, 1/K<sub>G</sub> is the reciprocal of the Kurtosis and  $\phi/ K_G$  and Sk/K<sub>G</sub> represents the ratio of mean versus kurtosis and skewedness versus kurtosis

The variation in values of  $\phi$ ,  $\sigma_1$ ,  $Sk_1$  and  $K_G$  along depth profile are comparable across each parameter. The present study uses  $\phi$ ,  $\sigma_1$ ,  $Sk_1$  and  $K_G$  to divide sedimentary sequence into 7 units along 800 cm thick sequence viz., (from bottom to top) Lithounit 1 (0-114 cm)- Sandy; Lithounit 2 (116-150 cm)- Muddy; Lithounit 3 (154-192 cm)- Sandy; Lithounit 4 (194-216 cm)-Muddy; Lithounit 5 (218-292 cm)-Sandy; Lithounit 6 (294-600 cm)-Sandy and Muddy; Lithounit 7 (602-800 cm)-muddy.

The plots  $Sk_1-Sk_2$ ,  $K_{G1}-K_{G2}$ ,  $\phi/K_G$ ,  $1/K_G$  and  $Sk_1/K_G$  (Figure 5-) signify relative change as well as relatively elevation (higher or lower topography) at the time of deposition of sediments. The  $\phi/K_G$  ratio suggests  $St_{MS+FS+CS}$  facies (Figure 5-7; from 0 to 120 cm),  $St_{MS+FS+CS}$  sub facies and  $St_{MS+CS}$  sub facies (Figure 5-7; from 145 to 350 cm) was deposited at lower elevation. Whereas  $F_{MSILT+VFS}$  (T) sub facies (from 120 cm to 145 cm and 365 cm) and  $F_{MSILT+VFS}$  (O) sub facies along with  $F_{MSILT+VFS+FS}$  sub facies deposited above 610 cm relatively at higher elevation within the channel. The sub facies  $Sm_{FS+MS}$  and  $Sl_{FS+VFS}$  dominate from 410 cm to 600 cm occur at transition elevation compared to other discussed sediment facies. The ratios of  $Sk_1/K_G$  and  $1/K_G$  further distinguish between  $St_{MS+FS+CS}$  sub facies and  $St_{MS+CS}$  sub facies suggesting that  $St_{MS+CS}$  sub facies were deposited at relatively higher elevation than  $St_{MS+FS+CS}$  sub facies. Possibly the  $St_{MS+CS}$  sub facies represent accumulation of coarser facies during high energy condition or a lag belonging  $St_{MS+FS+CS}$  sub facies resulted due to removal of finer sand under high energy conditions.

## 5.7 Discussion

The Late Holocene sediment sequence (802 cm thick) under present study, along the southern bank of Narmada, west of Kavery River, near village Uchediya represents a flood plain, the most conspicuous landform that get submerge in the monsoon season during floods. The sequence comprises of suites of seven sub facies that intercalate each other. The suites of sub facies are primarily decoded

applying cluster analysis of high resolution granulometric record supplemented with field sedimentological data at same resolution. The sub facies are further distinguished along bivariate asserting hydrodynamics. The plots of ratios of few statistical parameters along depth were used to decipher relative changes and position during deposition.

The conditions prior to initiation of sediment deposition are inferred from plots viz., M/K ratio, S/K ratio and 1/K ratio. The plots suggest the sediments were deposited at relatively lower elevation compared to overlying Fm<sub>SILT+VFS</sub> (T). The present study further infers that the St<sub>MS+FS+CS</sub> sub facies were deposited in a shallow channel environment. Cross trough structures and pebbles embedded with them suggest sediment was transported under traction as bed load. The shift in the thalweg line exposed the channel bed. High tidal influx deposited Fm<sub>SILT+VFS</sub> (T) sub facies with a sharp contact with adjacent previously deposited channel facies. Further changes in channel reinstated channel conditions. Sandwich of St<sub>MS+CS</sub> sub facies within St<sub>MS+FS+CS</sub> sub facies suggest accumulation of coarser sediment or erosion of finer sediment under flood conditions. Shift in thalweg line changes the permanent channel away from the present site of deposit. Intercalation of Fm<sub>SILT+VFS</sub> (T) and Fm<sub>SILT+VFS+FS</sub> shows mixed depositional environment tidal and overbank flood deposits. Further aggradations resulted in prominent point bar depositing Sl<sub>FS+VFS</sub> sub facies. Interaction of Fm<sub>SILT+VFS</sub> (O), Sl<sub>FS+VFS</sub> sub facies and Sm<sub>FS+MS</sub> sub facies thereafter suggest point bar accretion and stabilization. Finally the point bar bounded the southern bank of channel during non-monsoonal phases. During monsoonal floods submerged the point bar and depositing Fm<sub>SILT+VFS+FS</sub> sub facies capped with thin Fm<sub>SILT+VFS</sub> (O) as observed to present time. Numerous floods over a period accreted 200 m of over bank deposit. The landform thus accreted bounds the southern bank of present Narmada channel.

## **5.8 Inferences**

1. High resolution quantitative granulometric record gives significant number of sample population to decode suite of sediment facies and gives significant understanding within facies and their transitions.
2. The quantitative variations in various bivariant plots and ratio of different statistical parameters against depth distinguish textural characteristics of the facies and changes occurred prior the deposition of facies.
3. The exposed eight meter section at the southern bank of present Narmada channel preserves evidence of multi-process evolution for the landform.
4. The present high resolution analysis clearly brings out the seven stages for the aggradation of the sequence represented by individual facies. Whereas
5. Accretion of the Holocene depositional surface of the area can be grouped into two main environments, viz., a catastrophic fluvial environment and a tide dominated marine environment.
6. Change in the sedimentological characteristics of the Holocene surface can be interpreted as a result of major geomorphic change within the channel, which may be due to a catastrophic event of flood possibly accelerated by a climatic variability.